

Research article

Biogenic synthesis, characterization and effects of Mn-CuO composite nanocatalysts on Methylene blue photodegradation and Human erythrocytes

Carlos N. Kabengele¹, Giresse N. Kasiama¹, Etienne M. Ngoyi¹, Clement L. Inkoto², Juvenal M. Bete¹, Philippe B. Babady¹, Damien S. T. Tshibangu¹, Dorothée D. Tshilanda¹, Hercule M. Kalele¹, Pius T. Mpiana¹ and Koto-Te-Nyiwa Ngbolua^{2,3,*}

¹ Department of Chemistry, Faculty of Sciences, University of Kinshasa, B.P. 190, Kinshasa XI, Democratic Republic of the Congo

² Department of Biology, Faculty of Sciences, University of Kinshasa, B.P. 190, Kinshasa XI, Democratic Republic of the Congo

³ Department of Basic Sciences, Faculty of Medicine, University of Gbado-Lite, P.O. Box 111, Gbado-Lite, Democratic Republic of the Congo

* **Correspondence:** Email: jpnbolua@unikin.ac.cd; Tel: +243828239215.

Abstract: Each year more than 150,000 tons of dyes are released in effluents by industries. These chemicals entities non-biodegradable and toxic can be removed from effluent by metallic nanomaterials. The aqueous extract of *Manotes expansa* leaves is used as reducing and stabilizing agent in the biogenic synthesis of Mn-CuO nanocomposites. The nanoparticles obtained were characterized using UV-visible spectroscopy, X-ray Diffraction (XRD), X-ray Fluorescence, Dynamic Light Scattering (DSL), and Scanning Electron Microscopy (SEM). The hemotoxicity of biosynthesized nanomaterials was assessed by evaluating their hemolytic activity using erythrocytes as a model system. The photocatalytic activity of Mn-CuO was carried out by photocatalytic degradation of Methylene Blue dye as a model. The results obtained by UV-vis spectroscopy showed a Plasmonic Surface Resonance band at 408 nm. XRD and X-ray fluorescence made it possible to identify the presence of particles of formula $Mn_{0.53}Cu_{0.21}O$ having crystallized in a Hexagonal system ($a = 3.1080 \text{ \AA}$ and $c = 5.2020 \text{ \AA}$). Spherical morphology and average height $49.34 \pm 6.71 \text{ nm}$ were determined by SEM and DSL, respectively. The hemolytic activity of biosynthesized nanomaterials revealed that they are not hemotoxic in vitro (% hemolysis 3.2%) and 98.3% of Methylene Blue dye

was removed after 120 min under irradiation with solar light in the presence of Mn-CuO nanocomposites.

Keywords: Manganese; copper; nanocomposites; *Manotes expansa*; Methylene blue

1. Introduction

Around the world, approximately 700,000 tons of organic dyes are produced each year. 12% of these are lost in effluents during their manufacturing and 20% are discharged into wastewater after use. In total, an estimated quantity of around 150,000 tons of dyes is released each year in effluents by industries [1,2]. In the marine environment, these dyes form a layer on the surface of the water, thereby reducing the amount of oxygen needed for underwater life. Apart from that, organic dyes are known to cause many harmful effects on human health and plants when released into the environment. They are generally poisonous, carcinogenic and non-biodegradable [3]. The elimination of these toxic substances in industrial effluents has become a major public health and environmental problem due to their high chemical stability and resistance to conventional methods. Various techniques have been suggested for removing organic dyes from water, among these techniques, heterogeneous photocatalysis is much more advantageous [4]. This method involves the use of a semiconductor whose energy gap of the forbidden zone corresponds to the energy of the used light source. It is very fast and often leads to the complete mineralization of dye treated by oxidation at room temperature. However, most of the catalysts used absorb only UV radiation because of their wide band gap energy. Therefore, one of the major challenges in heterogeneous photocatalysis remains the development of new generation photocatalytic materials for high performance and especially active in the visible region [5,6].

Faced to these challenges, nanotechnology, which represents a new world where the matter has properties very different from those it presents at the macroscopic scale is an alternative. Indeed, due to their varied and often novel properties, nanomaterials metals conceal diverse potentialities and their uses open up multiple prospects in many sectors of activity such as environment, health, automobile, construction, food and electronics. Among different types of metallic nanoparticles, manganese and copper have attracted the attention of many researchers because of their multiple applications in various fields [7,8]. Mn and Cu nanoparticles have been widely used in the degradation of several types of persistent organic dyes from contaminated waters. However, there is very little data in the literature on the combination of these two metals in the form of nanocomposites. Some studies carried out in this direction, especially those made by Iqbal and Pramothkumar on the effect of Mn doped CuO nanoparticles proved a strong relevant activities improvement, compared to undoped CuO nanoparticles. In fact, bimetalization generally leads to the improvement of the properties of the material following a synergistic effect or combination of the properties of two metals [9–12]. Manufactured using green methods, Mn-CuO NPs retain active chemical molecules on their surfaces improving their efficacy and properties in the medical and pharmaceutical fields [13]. So, studies are currently carried out to discover new biological entities (Plants, Algae, Microorganisms, etc.) that can be used in the synthesis of nanocomposite particles with desired properties while respecting environmental standards.

In this study, we present a green synthesis method for Mn-CuO nanocomposites using *Manotes*

expansa extract (*M.expansa*) as a reducing and stabilizing agent for the first time, their use in the environmental field as well as their hemotoxicity. *Manotes expansa* is a plant belonging to the *Cannaraceae* family and known for its many uses in traditional medicine. *M.expansa* leaves are rich in phenolic compounds that can play the role as reducing and stabilizing agents [14,15]. Mn-CuO nanoparticles biosynthesized were characterized using several techniques to confirm their presence. UV-visible spectrophotometry was used for the determination of the Resonance Plasmonic Surface band. The crystal system, lattice parameters and composition particle chemistry were determined using X-ray Diffraction and fluorescence X. As for the size and morphology of nanocomposites, Dynamic Diffusion measurements of Light (DSL) and Scanning Electron Microscopy (SEM) were performed.

2. Materials and methods

2.1. Reagents

The chemicals used in this study such as Mn (CH₃COO)₂ 2H₂O, CuSO₄ 5H₂O, and Methylene Blue were provided by Sigma Aldrich. Hydrochloric acid, sodium hydroxide, all analytical grades were supplied by Merck, while Bi-distilled water was used in the preparation of solutions.

2.2. Preparation of extracts

Plant material consists of *M.expansa* leaves which were collected in Kinshasa, and identified at the herbarium of the National Institute of Agronomic Studies and Research (INERA) of Kinshasa. These leaves were washed with water to remove dust, dried at room temperature and protected from sunlight, then reduced to powder using a Sinbo type grinder. 50 g of powders were macerated in 500 mL of bi-distilled water, stirred and left at room temperature for 24 h. Then, the mixture was heated at 50 °C and stirred for 2 h, filtered and kept in the fridge at 4 °C for later use.

2.3. Biosynthesis of Mn-CuO nanocomposites

The experimental procedure described by Ahmad was used for the biogenic synthesis of Mn-CuO nanocomposites with slight modifications [9]. Briefly, 100 mL of 0.01 N solution of CuSO₄ 5H₂O were mixed with 0.01 N Mn (CH₃COO)₂ 2H₂O (volume ratio 1:1) and the mixture obtained was stirred at room temperature for 5 min to have a homogeneous mixture of precursor salts. Then, 20 mL of the aqueous extract of *M.expansa* leaves was added with thermal stirring at 60 °C and 1,000 rpm. After 30 min of stirring, the change in color from blue-green to mauve denotes the start of metal ions precipitation in nanoparticles. The nanomaterials obtained were centrifuged at 4,000 rpm and washed 3 times with bi-distilled water to remove impurities, then calcined at 300 °C and stored at 4 °C for characterization. The optimal synthesis parameters were fixed by varying the extract concentration, the pH and the temperature of the medium during the synthesis. A 0.01 N solution of NaOH and 0.01 N HCl were used to modify the pH of the medium.

2.4. Characterization of nanocomposites

The Surface Resonance Plasmonic (SRP) of Mn-CuO nanomaterials was determined by wavelength scan ranging from 200 to 700 nm using a JENWAY 7315 UV-visible spectrophotometer. A Scanning Electron Microscope TESCAN Lyra 3 was used to determine the morphology of synthesized particles. The average particle size was determined by Dynamic Light Scattering (DSL). As for the crystalline structure and the chemical composition of the synthesized nanocomposites, a PHYWE 4.0 X-ray diffractometer using Cu K α ($\lambda = 1.540596 \text{ \AA}$) with 2θ angle varied from 20 to 90 ° and an X-ray spectrophotometer were used.

2.5. Photocatalytic degradation of Methylene blue

The photocatalytic activity of Mn-CuO nanocomposites was evaluated by the degradation of an aqueous solution of Methylene Blue at room temperature and under solar irradiation. 100 mL of Methylene blue solution with an initial concentration of 10 mg/L was mixed with 10 mg of nanocatalysts under stirring in the absence of light for 30 min for a homogeneous distribution of catalyst in the medium and for reaching the Adsorption-desorption equilibrium at nanomaterials surface. The mixture was irradiated under sunlight for 2 h 30 and after each 30 min, an aliquot (2 mL) was taken, and centrifuged at 10,000 rpm using an R-BC Laboratory Centrifuge. The filtrate obtained was analyzed by a JENWAY 7315 UV/Visible spectrophotometer at 663 nm to determine the degree of discoloration.

2.6. Hemolytic activity of Mn-CuO nanoparticles

Human blood taken from a healthy donor was used to prepare the erythrocyte suspension for hemolytic power of nanocomposites in vitro evaluation. The experimental protocol described by Chen et al. was used in this work [16].

3. Results and discussion

3.1. Synthesis and characterization of nanocomposites

3.1.1. Synthesis

Generally, the color change during nanoparticle synthesis using plant extracts is an important factor that confirm their formation in the medium [17,18]. Figure 1 below shows the color change due to the formation of Mn-CuO nanoparticles in the solution.

After 40 min of reaction at 60 °C, the solution turns from dark green to mauve, which implies the nanoparticles formation in the solution. At this stage, nanoparticles are not yet stabilized, it is the reduction and nucleation phase, initiated often by flavonoids and terpenoids present in plant leaves [19,20]. After 90 min, the color of solution turns brown tending towards red, this color persisted for up to 120 min, thus confirming the stabilization of nanoparticles in the medium. In fact, the secondary metabolites present in the leaves of *Manotes expansa* play the role of reducer and stabilizer.



Figure 1. Synthesis of nanoparticles in solution.

3.1.2. Characterization of nanocomposites

(1) Characterization of nanocomposites by UV-visible spectroscopy

The SRP band of Mn-CuO nanocomposites was determined by UV-visible spectroscopy. Indeed, when incident light resonates with conduction band electrons on the surface of nanoparticles, it causes absorption at a characteristic wavelength that can be used to identify particles [21]. Figure 2 above gives the UV-visible spectrum of the mixture of precursor salts and extract of *Manotes expansa* after 2 h of contact.

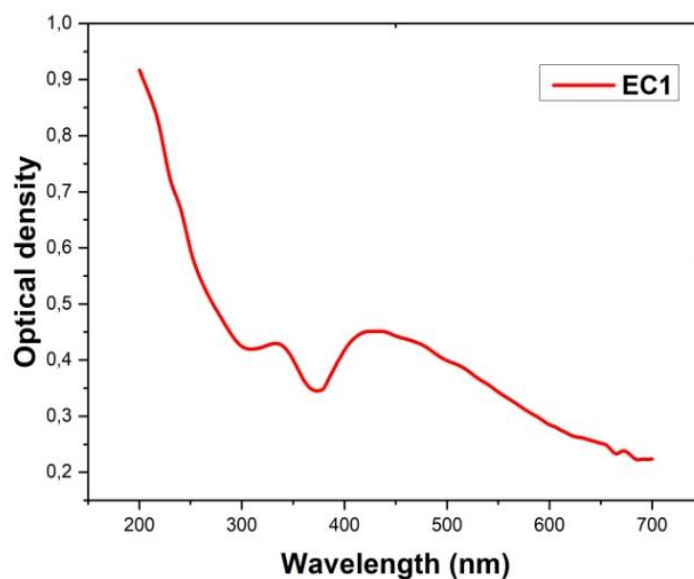


Figure 2. UV-visible spectrum of Mn-CuO nanocomposites.

(2) Synthesis optimization

The synthesis optimization parameters were fixed by successive variation of temperature, pH of the medium and concentration of the extract.

(a) Optimal temperature

The temperature is one of the essential parameters in green synthesis because of its capacity to modify the optical properties of particles at the nanometric scale. The characteristic absorbance was measured at different temperature values, namely 40 °C, 60 °C, 80 °C and 100 °C. Figure 3 below gives the influence of temperature on Mn-CuO nanocomposites synthesis.

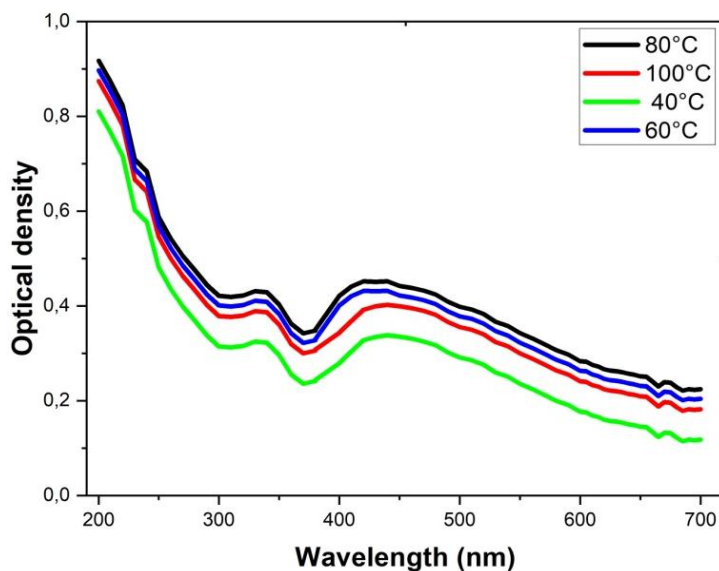


Figure 3. Effect of temperature on Mn-CuO synthesis.

From the foregoing, it can be seen that the change in color already occurs at 5 min when the temperature is set at 80 °C, indicating that the rate of synthesis increases with the temperature of the medium.

During this study, we also noticed that the temperature also slightly modifies the absorption band due to the PSR of Mn-CuO nanocomposites. At 40 °C, a slight Redshift is observed, the maximum absorption wavelength is 418 nm while from 60 °C and 80 °C the PSR band is located at 409 nm, this confirms the influence of temperature on particle morphology and size. Indeed, the increase in temperature leads to the formation of stable particles of small sizes which absorb at low wavelengths [22]. From 100 °C, the absorbance significantly decreases, this can be explained by the fact that at this temperature, most of the secondary metabolites present in the leaves of *Manotes expansa* deteriorate and these metabolites are no longer available to fulfill their role [20]. The temperature of 80 °C can be considered the optimum temperature in the synthesis of Mn-CuO nanocomposites.

(b) Optimal pH

The pH controls the activity of the functions of molecules present in plant which in turn determines the rate of reduction of the metal salt and the stability of the nanoparticles [23]. Figure 4 below gives the influence of pH on the synthesis of Mn-CuO nanocomposites.

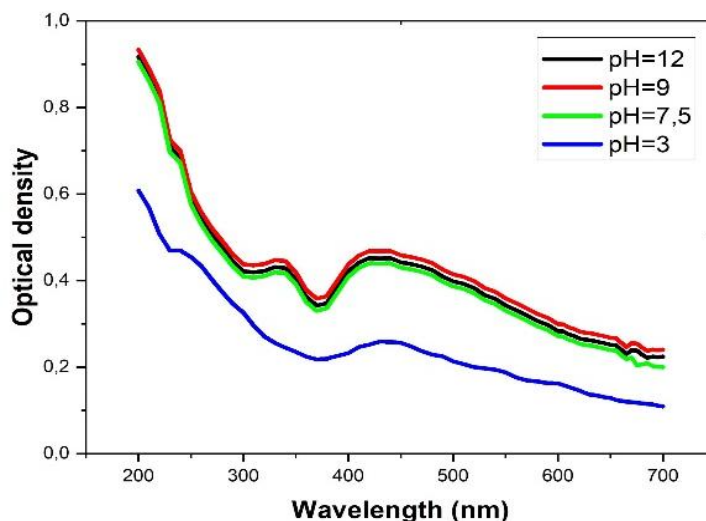


Figure 4. pH effect on synthesis of Mn-CuO.

When the pH of the medium is acidic, the rate of formation decreases significantly to the point that after 90 min, only a very small quantity of Mn-CuO particles is produced. This decrease in speed is proven by a low absorbance at the characteristic wavelength of nanocomposites (Figure 3). Therefore, it was found that the reduction and nucleation of metal ions increase with the pH of the medium as in most cases [24]. In the present study, pH 9 constitutes the optimum value beyond which no increase was observed.

(c) Volume of extract

Figure 5 below shows the influence of the salt/extract volume ratio on the synthesis of nanocomposites at 80 °C.

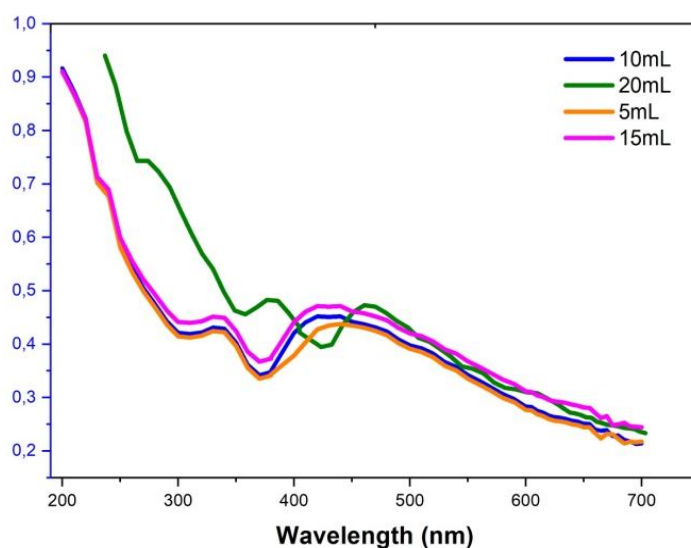


Figure 5. Effect of extract concentration on the synthesis of Mn-CuO nanoparticles.

It appears from this result that the variation in the volume of *M.expansa* extract has more influence on the size and morphology of nanocomposites than on their concentration. The addition of 10 mL and 15 mL of *Manotes expansa* extract causes a blue shift due to the formation of small particles. Increasing the volume of the extract up to 20 mL causes a redshift which may be associated with the production in the medium of nanoparticles of much larger size and which tend towards agglomeration. In fact, when the size and the diameter of the particles increase, the energy necessary for the excitation of the Plasmonic surface of particles decreases, one observes a shift towards large values of wavelength [20,25].

(3) Chemical composition of nanocomposites

In order to determine the crystal structure, lattice parameter and space group of prepared nanocomposites, an X-ray 4.0 PHYWE type diffractometer was used. The result shows that the composition of nanocomposites is $Mn_{0.53}Cu_{0.21}O$ which crystallized in a Hexagonal crystalline system having as lattice parameter $a = 3.1080 \text{ \AA}$, $c = 5.2020 \text{ \AA}$, then the calculated density $\rho = 5.027 \text{ g/cm}^3$. Figure 6 and Table 1 below present respectively the XRD spectrum and its summary.

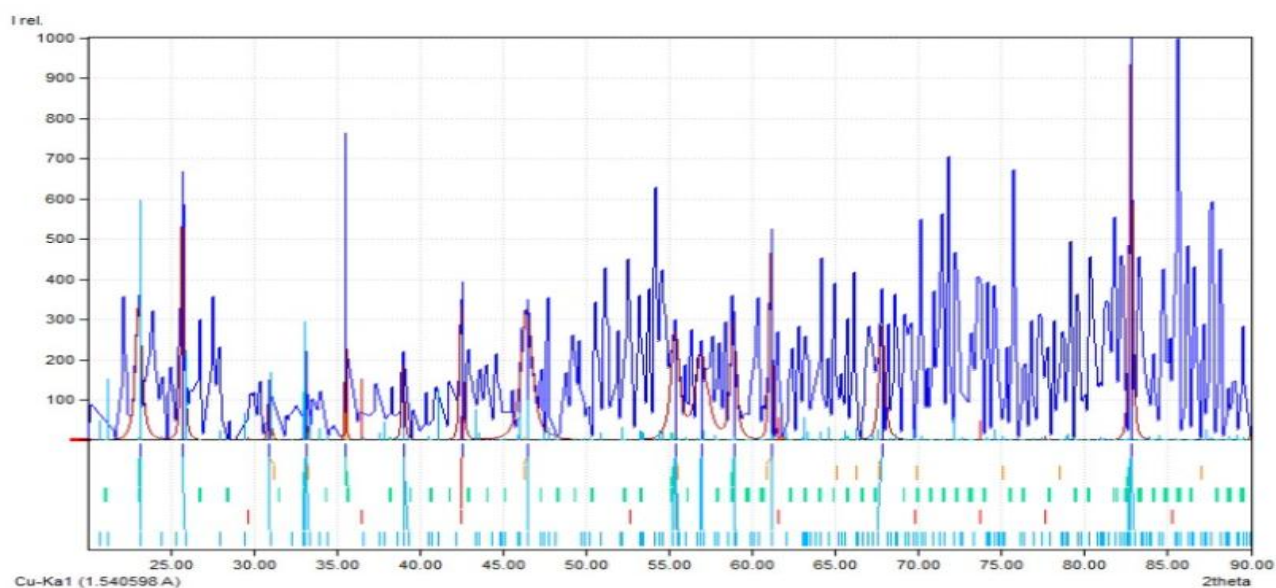


Figure 6. XRD pattern of Mn-CuO nanocomposites.

Table 1. X-ray diffraction peak values of Mn-CuO nanocomposites.

No	2theta (°)	(\AA)	I/I_0	Counts (peak area)	FWHM
4	33.20	2.6963	220.99	0.29	0.1000
5	35.56	2.5228	762.05	0.63	0.0625
8	46.49	1.9520	348.00	3.66	0.8007
12	61.17	1.5139	523.54	1.43	0.2077
14	82.81	1.1647	1000.00	2.90	0.2210

The peaks at angles 2θ equal 82.81° ; 61.17° ; 46.49° ; 35.56° ; 33.20° were associated with Mn-CuO nanoparticles. The elementary chemical analysis of nanoparticles made it possible to identify the presence of Cu-K α , Cu-K β and a peak of Mn. The spectrum is depicted in Figure 7 below.

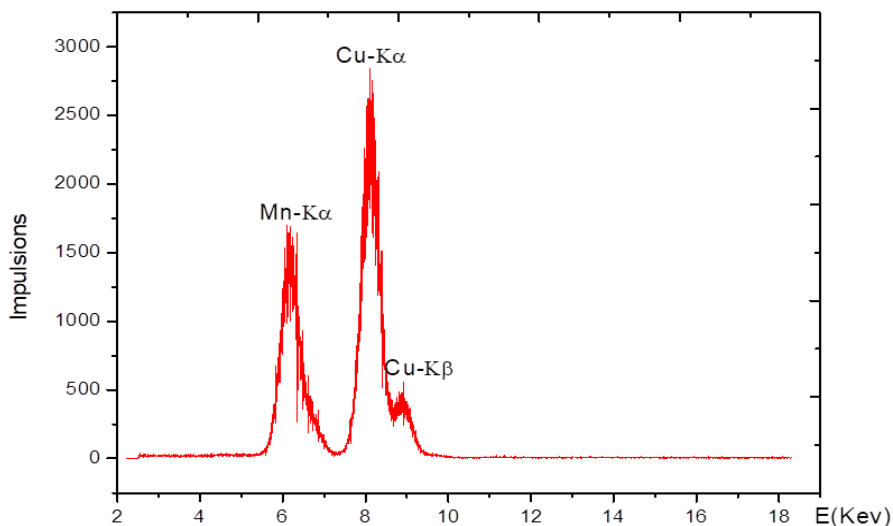


Figure 7. X-ray spectrum of NPs Mn-CuO.

The dominant morphology remains spherical for Mn-CuO nanoparticles in Figure 8 below. The large particles in this figure explain the agglomeration of particles due to a long storage period, since the SEM measurements were carried out 8 months after synthesis. Indeed, nanoparticles are very reactive because of their sizes and their surface properties. They tend to agglomerate to form particles of much larger sizes, which makes their long-term preservation difficult [26]. The DSL measurement in Figure 9 gave an average size of the particles estimated at 49.34 ± 6.71 nm, this confirms the formation of particles of sizes less than 100 nm.

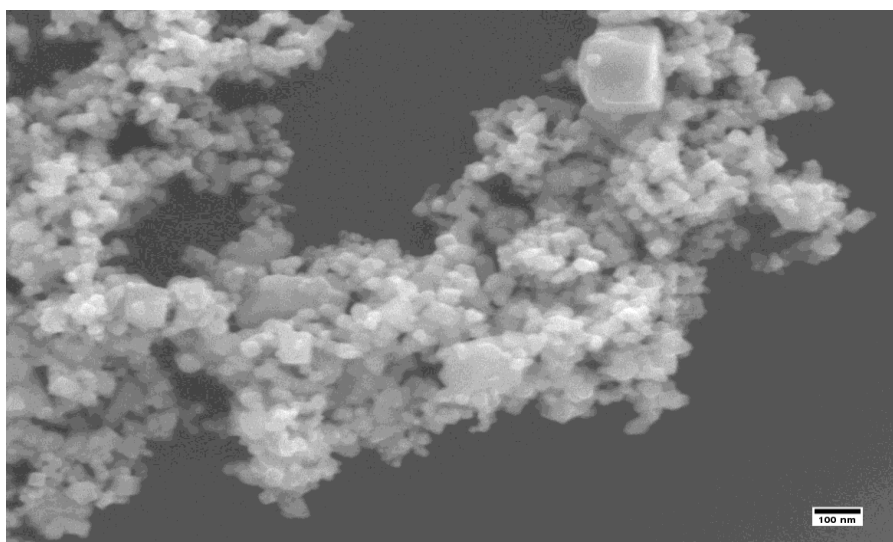


Figure 8. Morphologie des nanoparticules de Mn-CuO.

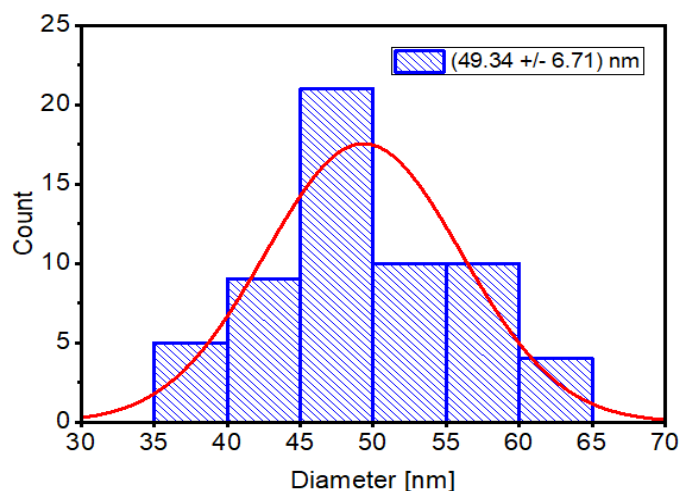


Figure 9. Distribution de la taille moyenne des nanoparticules Mn-CuO.

3.2. Photocatalytic degradation of Methylene blue

3.2.1. Adsorption of Methylene blue on the surface of nanomaterials

The contribution of the adsorption phenomenon in dye elimination was evaluated. After bringing Mn-CuO nanocomposites into contact with Methylene blue under magnetic stirring at 1,000 rpm, the absorbances were measured at different times in the absence of light and at room temperature. Figure 10 below gives the evolution of the concentration of methylene blue in the presence of Nps of Mn-CuO in the dark as a function of time.

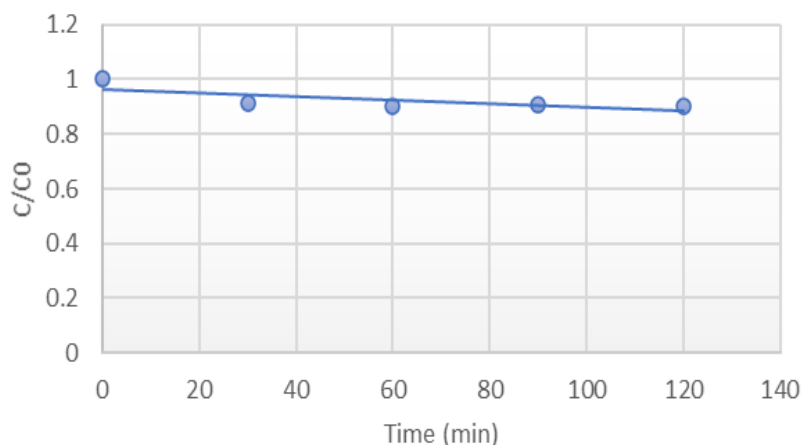


Figure 10. Adsorption of MB dye on nanocomposites surface.

A slight decrease in the initial concentration of Methylene blue was observed during the first 30 min. This time is necessary to reach the adsorption-desorption equilibrium in the medium, ie all the adsorbent pores on the surface of the Nps Mn-CuO are occupied by at least one molecule of Methylene blue. This has also been noticed in several studies on the adsorption of organic pollutants on nanoparticles [27,28]. The degree of discoloration after 2 h of contact was 12.5%.

3.2.2. Photocatalytic activity of Mn-CuO nanocomposites

Visible light plays important role in the excitation of the Plasmonic Surface Resonance of nanoparticles, and therefore determines the production of reactive species in solution. A JENWAY type UV-visible spectrophotometer was used to monitor the photocatalytic degradation of Methylene blue in the presence of Mn-CuO nanoparticles as a function of time. Figure 11 below shows the evolution of discoloration of water polluted with Methylene Blue in the presence of nanocatalysts as a function of the time of exposure to the sun.

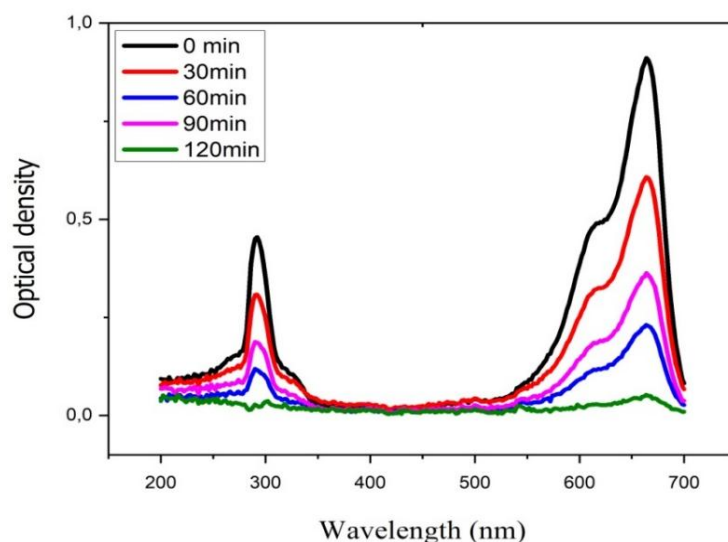


Figure 11. Photocatalytic degradation of Methylene blue using Mn-CuO NPs as a function of time.

From above, it can be seen that the elimination of MB in solution depends on the time of exposure to the sun. After 120 min, the entire quantity of Methylene blue initially present in the medium has been degraded (totally mineralized) in the presence of nanocatalysts and light. The discoloration rate calculated after 2 h being 98.3% seems far superior to that found in the absence of light; which makes it possible to confirm the photocatalytic nature of Mn-CuO nanoparticles. This result corroborates with that of Chanu et al. who worked on the photocatalytic degradation of BM in the presence of Mn/ZnO nanocomposites [29]. Thus, biosynthesized nanomaterials have high photocatalytic activity and can be used in the degradation of persistent organic pollutants in the environment.

3.3. Hemolytic effect

The determination of hemolytic effect is one of the most used tests to study the interaction of nanomaterials with blood constituents [30]. Due to their size of less than 100 nm, nanoparticles can pass through skin pores and end up in the bloodstream. Since most of them are known to induce significant cytotoxicity, then it was necessary to study their toxicity in blood [31]. After contact of 20 $\mu\text{g/mL}$ of the nanocomposites with the blood, the percentage of hemolysis induced was approximately 3.2%, which remains below the threshold of 5%. Indeed, according to the criterion of

the ASTM E252408 standard, a percentage of hemolysis greater than 5% indicates that the nanomaterials tested damage the red blood cells. Thus, for a nanomaterial concentration of 20 $\mu\text{g/mL}$, the hemolysis percentage of 3.2% found allowed us to conclude that Mn-CuO nanocomposites are not hemotoxic [32].

4. Conclusion

The present study gives a much simpler way for the synthesis of composite Mn-CuO nanoparticles using the aqueous extract of *Manotes expansa* leaves, a plant rich in phenolic compounds capable of reducing and stabilizing Cu^{2+} and Mn^{2+} ions into nanoparticles. UV-visible spectroscopy made it possible to identify the characteristic absorption band of nanoparticles (Mn-CuO). The size and morphology of the particles were determined respectively by Dynamic Light Scattering (DSL) and Scanning Electron Microscopy (SEM). SEM images showed a dominant rectangular morphology having an average size of 49.34 ± 6.71 nm. X-ray diffraction and fluorescence confirmed the presence of Mn-CuO. The nanocomposites produced were used in solar photocatalysis for the degradation of the methylene blue dye. It appears from this study that the Mn-CuO nanoparticles are very active in the presence of sunlight and 98.3% of the dye has been destroyed after 2 h of contact. Thus, this nanotechnological approach makes it possible to depollute effluents contaminated by toxic chemical substances, which help in environmental protection and promote the good health as well as the well-being of the population.

In perspective, some points remain to be deepened, it would therefore be interesting to complete this study by using FTIR spectroscopy to elucidate the structure of molecules directly involved in the reduction and stabilization of Mn-CuO nanocomposites. This gives us an idea about the mechanism.

Conflicts of interest

The authors declare no conflict of interest.

References

1. Pinheiro LRS, Gradissimo DG, Xavier LP, et al. (2022) Degradation of azo dyes: Bacterial potential for bioremediation. *Sustainability* 14: 1510. <https://doi.org/10.3390/su14031510>.
2. Rauf MA, Ashraf SS (2009) Review: Fundamental principles and application of heterogeneous photocatalytic degradation of dyes in solution. *Chem Eng J* 151: 10–18. <https://doi.org/10.1016/j.cej.2009.02.026>
3. Zhuang Y, Zhu Q, Li G, et al. (2022) Photocatalytic degradation of organic dyes using covalent triazine-based framework. *Mater Res Bulletin* 146: 111619. <https://doi.org/10.1016/j.materresbull.2021.111619>.
4. Sibhatu AS, Weldegebriela KG, Sgaradevan S (2022) Photocatalytic activity of CuO nanoparticles for organic and inorganic pollutants removal in wastewater remediation. *Chemosphere* 300: 134623. <https://doi.org/10.1016/j.chemosphere.2022.134623>
5. Fouda A, Salam S, Wassel AR, et al. (2020) Optimization of green biosynthesized visible light active CuO/ZnO nano-photocatalysts for the degradation of organic methylene blue dye. *Helion* 6: e04896. <https://doi.org/10.1016/j.helion.2020.e04896>.

6. Lacombe S, Tran-thi T, Guillard C, et al. (2007) La photocatalyse pour l'élimination des polluants. *Actualités chimiques* 308: 79–93.
7. Liu X, Chen C, Zhao Z, et al. (2013) A review on the synthesis of manganese oxide nanomaterials and their applications on lithium-ion batteries. *J Nanomater* 2013: 736375. <http://dx.doi.org/10.1155/2013/736375>
8. Naika HR, Lingaraju K, Manjunath K, et al. (2015) Green synthesis of CuO nanoparticles using *Gloriosa superba* L. extract and their antibacterial activity. *J Taibah Univ Sci* 9: 7–12. <https://doi.org/10.1016/j.jtusci.2014.04.006>.
9. Ahmad MM, Kotb HM, Mushta S, et al. (2022) Green synthesis of Mn + Cu bimetallic nanoparticles using *vinca rosea* extract and their antioxidant, antibacterial, and catalytic activities. *Crystals* 12: 72. <https://doi.org/10.3390/cryst12010072>.
10. Basavegowda N, Baek K (2021) Multimetallic nanoparticles as alternative antimicrobial agents: Challenges and perspectives. *Molecules* 26: 912. <https://doi.org/10.3390/molecules26040912>.
11. Iqbal M, Thebo AA, Shah AH, et al. (2016) Influence of Mn-doping on the photocatalytic and solar cell efficiency of CuO nanowires. *Inorg Chem Commun* 76: 71–76. <https://doi.org/10.1016/j.inoche.2016.11.023>.
12. Pramothkumar A, Senthilkumar N, Mercy Gnana Malar KC, et al. (2019) A comparative analysis on the dye degradation efficiency of pure, Co, Ni and Mn-doped CuO nanoparticles. *J Mater Sci-Mater El* 30: 19043–19059. <https://doi.org/10.1007/s10854-019-02262-4>.
13. Vindhya PS, Kavitha VT (2022) Leaf extract-mediated synthesis of Mn-doped CuO nanoparticles for antimicrobial, antioxidant and photocatalytic applications. *Chem Pap*. <https://doi.org/10.1007/s11696-022-02631-0>.
14. Kabengele CN, Kasiama GN, Ngoyi EM, et al. (2022) Secondary metabolites and mineral elements of *Manotes expansa* and *Aframomum albviolaceum* leaves collected in the democratic republic of Congo. *ARRB* 37: 57–63.
15. Rizwana H, Alwhibi MS, Al-Judaie RA, et al. (2022) Sunlight-mediated green synthesis of silver nanoparticles using the berries of *Ribes rubrum* (Red Currants): characterization and evaluation of their antifungal and antibacterial activities. *Molecules* 27: 2186. <https://doi.org/10.3390/molecules27072186>.
16. Chen LQ, Li Fang, Ling J, et al. (2015) Nanotoxicity of silver nanoparticles to red blood cells: size dependent adsorption, uptake, and hemolytic activity. *Chem Res Toxicol* 28: 501–509. <https://doi.org/10.1021/tx500479>
17. Pandey S, Singh S (2020) Eco-friendly nanocomposite and properties of manganese nanoparticles using UV-vis and IR fourier spectrum. *IJISRT* 5: 770–773.
18. Shah M, Fawcett D, Sharma S, et al. (2015) Review green synthesis of metallic nanoparticles via biological entities. *Materials* 8: 7278–7308. <https://doi.org/10.3390/ma8115377>.
19. El-seedi, El-Shabasy RM, Khalifa SAM, et al. (2019) Metal nanoparticles fabricated by green chemistry using natural extracts: biosynthesis, mechanisms, and applications. *RSC Adv* 24539–24559. <https://doi.org/10.1039/C9RA02225B>
20. Makarov VV, Love AJ, Sinitsyna OV, et al. (2014) Green nanotechnologies: Synthesis of metal nanoparticles using plants. *Acta Naturae* 6: 35–44. <https://doi.org/10.32607/20758251-2014-6-1-35-44>

21. Desai R, Mankad V, Gupta SG, et al. (2012) Size distribution of silver nanoparticles: UV-visible spectroscopic assessment. *Nanosci Nanotechnol Let* 4: 30–34. <https://doi.org/10.1166/nnl.2012.1278>
22. Yeshchenko OA, Bondarchuk IS, Gurin VS, et al. (2013) Temperature dependence of the surface plasmon resonance in gold nanoparticles. *Surf Sci* 608: 275–281, <http://dx.doi.org/10.1016/j.susc.2012.10.019>.
23. Seifipour R, Nozari M, Pishkar L (2020) Green synthesis of silver nanoparticles using *Tragopogon Collinus* leaf extract and study of their antibacterial effects. *JIOPM* 30: 2926–2936. <https://doi.org/10.1007/s10904-020-01441-9>
24. Vidhu VK, Aromal SA, Philip D (2011) Green synthesis of silver nanoparticles using *Macrotyloma* uniform. *Spectrochim Acta A* 83: 392–397. <https://doi.org/10.1016/j.saa.2011.08.051>
25. Berta L, Coman NA, Rusu A, et al. (2021) A review on plant-Mediated synthesis of Bimetallic nanoparticles, characterization and their biological applications. *Materials* 14: 7677. <https://doi.org/10.3390/ma14247677>
26. Pinto VV, Ferreira MJ, Silva R, et al. (2010) Long time effect on the stability of silver nanoparticles in aqueous medium: effect of synthesis and storage conditions. *Colloid Surface A* 364: 19–25. <https://doi.org/10.1016/j.colsurfa.2010.04.015>
27. Azeez F, Al-Hetlani E, Arafa M (2018) The effect of surface charge on photocatalytic degradation of Methylene Blue dye using chargeable titania nanoparticles. *Sci Rep* 2018: 7104. <https://doi.org/10.1038/s4158-018-15673-5>.
28. Taylor MG, Augustin N, Gounaris CE, et al. (2015) Catalyst design based on morphology and environment dependent adsorption on metal nanoparticles. *ACS Catal* 20155: 6296–6301. <https://doi.org/10.1021/acscatal.5b01696>
29. Chanu LA, Singh WJ, Singh KJ, et al. (2019) Effect of operational parameters on the photocatalytic degradation of Methylene blue dye solution using manganese doped ZnO nanoparticles. *Results Phys* 12: 1230–1237. <https://doi.org/10.1016/j.rinp.2018.12.089>
30. Dobrovolskaia MA, Clogston JD, Neun BW (2008) Method for analysis of nanoparticle hemolytic properties in vitro. *Nano Lett* 8: 2180–2187. <https://doi.org/10.1021/nl0805615>
31. Gabor F (2011) Characterization of nanoparticles intended for drug delivery. *Sci Pharm* 79: 701–702.
32. Gul A, Shaheen A, Ahmad I, et al. (2021) Green synthesis, characterization, enzyme inhibition, antimicrobial potential, and cytotoxic activity of plant mediated silver nanoparticle using *Ricinus communis* leaf and root extracts. *Biomolecules* 11: 206. <https://doi.org/10.3390/biom11020206>.



AIMS Press

© 2023 the Author(s), licensee AIMS Press. This is an open access article distributed under the terms of the Creative Commons Attribution License (<http://creativecommons.org/licenses/by/4.0>)